On estimation of diffusion coefficient based on spatio-temporal FRAP images:

An inverse ill-posed problem

Radek Kaňa[♠], Ctirad Matonoha[♡],
Štěpán Papáček[♣], Jindřich Soukup[♣]

[♠]Institute of Microbiology, AS CR, Opatovický mlýn, Třeboň
[♡]Institute of Computer Science, AS CR, Prague
[♣]SXS FFPW, University of South Bohemia, Nové Hrady

PANM 16, 3. - 8. června 2012, Dolní Maxov

FRAP technique

FRAP (Fluorescence Recovery After Photobleaching) technique allows detection of diffusivity of autofluorescence compound like proteins (e.g. phycobiliproteins) and also other non-fluorescence compound that are fluorescently tagged (e.g. green fluorescence proteins - GFP).

This method is based on application of short, intense laser irradiation (the so called bleach) to a small target region (Region Of Interest - ROI) of the cell that causes irreversible loss in fluorescence in this area without any damage in intracellular structures. After the "bleach" (or "bleaching"), the observed recovery in fluorescence in the "bleached area" reflects diffusion of fluorescence compounds from the area outside the bleach.

FRAP data: spatio-temporal image

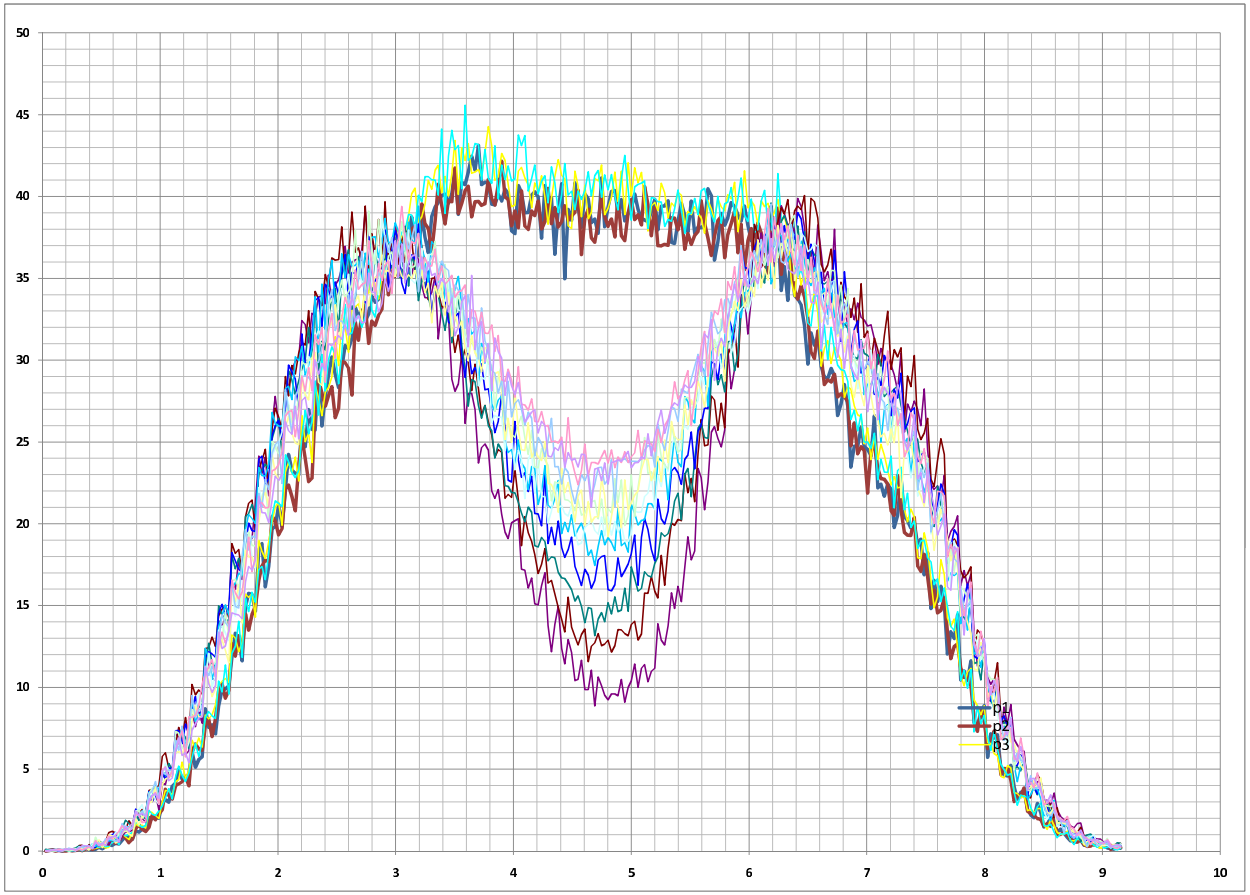

Fluorescence intensity (in arbitrary units) vs. Distance [μm].
Experimental data from FRAP experiment with red algae *Porphyridium cruentum* describing the phycobilisomes mobility on thylakoid membrane.

Outline

Outline

Our study describes the development and validation of a reliable method aiming to determine the phycobilisomes diffusivity on thylakoid membrane using FRAP experiments. This was usually done by experimental curve fitting to the analytical (closed form) models. For example, Moullineaux *et al.* have exploited the rotational symmetry of the cells by bleaching a plane across the short axis of the cell. Therefore, one-dimensional bleaching profiles along the long axis were generated.

C. W. Moullineaux supposed that:

1. $x \in \mathbb{R}$, i.e. the infinite domain
2. the initial bleaching profile is Gaussian: $y(x, t_0) = y_{0,0} \exp \frac{-2x^2}{{r_0}^2}$, where r_0 is the half-width of the bleach at time $t_0 = 0$, $y_{0,0}$ is the maximum depth at time t_0, i.e. the first post-bleach signal at the center ($x = 0$) subtracted from its pre-bleach level
3. boundary conditions correspond to the complete recovery: $y \to 0$ as $t \to \infty$, $y \to 0$ as $x \to \infty$.

C. W. Moullineaux method

The calculation of the diffusion coefficient D according to Moullineaux *et al.* resides in the weighted linear regression: a plot of $(\frac{y_{0,0}}{y(0,t)})^2$ against time, which should give a straight line with the tangent $\frac{8D}{{r_0}^2}$.

$$y(x,t) = \frac{y_{0,0}r_0}{\sqrt{{r_0}^2 + 8Dt}} \exp \frac{-2x^2}{{r_0}^2 + 8Dt}, \quad y(0,t) = \frac{y_{0,0}r_0}{\sqrt{{r_0}^2 + 8Dt}},$$

where $y(x,t)$ is the post-bleach signal at time t subtracted from the pre-bleach profile, $y(0,t)$ is the maximum depth at time t.

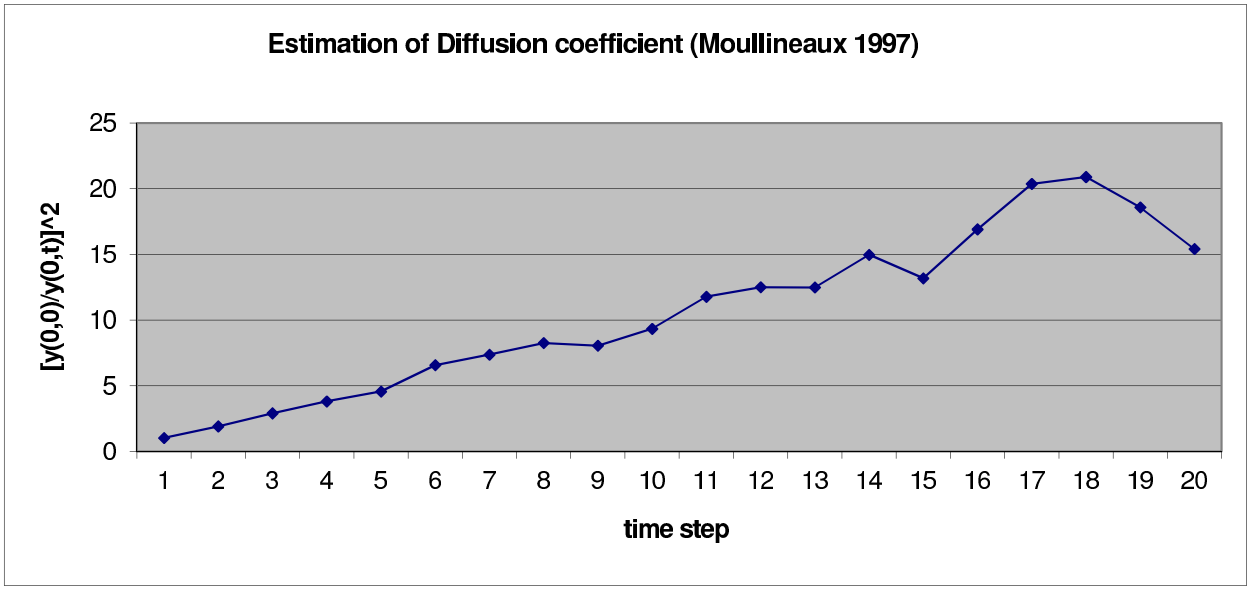

Diffusion-reaction equation

The recovery of unbleached particle concentration as a function of spatial coordinate r and time t is modeled with a linear, diffusion-reaction equation on a two-dimensional domain Ω:

$$\frac{\partial C}{\partial t} - \nabla \cdot (D \nabla C) = R(C) \tag{1}$$

- $C(r, t)$ is the unbleached particle concentration,
- D is the fluorescent particle diffusivity within the domain Ω (supposed to be a constant),
- $R(C)$ is a reaction term.

Reaction term $R(C)$ can be described as a first order reaction:

$$R(C) = -k_S \, C \tag{2}$$

- k_S is a rate constant describing bleaching during scanning.

Initial and boundary conditions

- The initial condition is

$$C_0(r) = f(r, t_0) \quad \text{in} \quad \Omega.$$

- The time varying boundary condition is
  - either of the Dirichlet type

$$C(r, t) = g(r, t) \quad \text{on} \quad \partial\Omega \times [t_0, T].$$

  - or of the Neumann type (based on 1^{st} Fick's law)

$$-D \nabla C(r, t) = h(r, t) \quad \text{on} \quad \partial\Omega \times [t_0, T].$$

The dimensionless form

If we adopt the form of reaction term according to (2) and introduce

- the dimensionless spatial coordinate $x \in [0, 1]$,
- the dimensionless diffusion coefficient $p > 0$,
- the dimensionless time $\tau \geq \tau_0$,
- the dimensionless normalized unbleached particle concentration y

by

$$x := \frac{r}{L}, \quad p := \frac{D}{D_0}, \quad \tau := t\,\frac{D_0}{L^2}, \quad y := \frac{C}{C_{pre}}, \tag{3}$$

where

- L is the length of our specimen in direction $\perp$ to bleach spot,
- D_0 is a constant with some characteristic value (unit: $\mathrm{m}^2\mathrm{s}^{-1}$),
- C_{pre} is a pre-bleach concentration of C,

we finally obtain the following form of dimensionless diffusion-reaction equation on one-dimensional domain, i.e. for $x \in [0, 1]$.

Outline

1D problem formulation

One-dimensional form of diffusion-reaction equation:

$$\frac{\partial y}{\partial \tau} - p\,\frac{\partial^2 y}{\partial x^2} = -\frac{k_S L^2}{D_0}\,y. \tag{4}$$

The initial condition is

$$y(x, \tau_0) = f(x), \quad x \in [0, 1]. \tag{5}$$

The time varying boundary conditions are either of the Dirichlet type

$$y(0, \tau) = g_0(\tau), \quad y(1, \tau) = g_1(\tau), \quad \tau \geq \tau_0, \tag{6}$$

or of the Neumann type

$$-p\,\frac{\partial y}{\partial x}(0, \tau) = h_0(\tau), \quad p\,\frac{\partial y}{\partial x}(1, \tau) = h_1(\tau), \quad \tau \geq \tau_0. \tag{7}$$

For the sake of clarity we further neglect the bleaching during scanning, i.e. we put $k_S = 0$ (the right-hand side in (4) is zero).

Experimental data

Based on FRAP experiments, we have a 2D dataset in form of a table with $(N+1)$ rows corresponding to the number of spatial points where the values are measured, and $(M+m+1)$ columns with m pre-bleach and $M+1$ post-bleach experimental values forming 1D profiles

$$y_{exp}(x_i, \tau_j), \quad i = 0 \dots N, \quad j = -m \dots M.$$

In fact the process is determined by

- m columns of pre-bleach data containing the information about the steady state and optical distortion
- $M+1$ columns of post-bleach data containing the information about the transport of unbleached particles (due to the diffusion) through the boundary

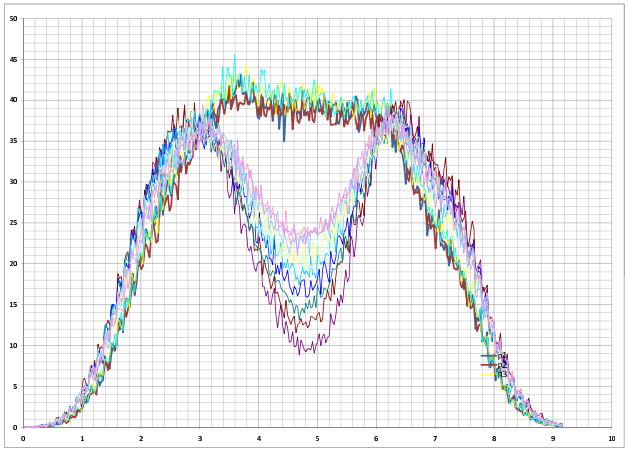

Re-scaling

Experimental values:

- space interval between first and last measurement points: $[a, b]$
- re-scaled dimensionless space interval: $x \in [0, 1]$
- length of space interval: $L = b - a$
- re-scaled distance between two space measurements: $h = \frac{1}{N}$
- time interval between two measurements: T
- re-scaled dimensionless time interval: $\tau_t = \frac{TD_0}{L^2}$

Re-scaled experimental data

Consequently,

$$x_0 = 0, \quad x_N = 1,$$

τ_0 corresponds to the first post-bleach measurement, and

- $y_{exp}(x_i, \tau_0),\ i = 0 \dots N$, represents the IC,
- $y_{exp}(0, \tau_j),\ j = 0 \dots M$, represents the left Dirichlet BC,
- $y_{exp}(1, \tau_j),\ j = 0 \dots M$, represents the right Dirichlet BC,
- the Neumann BC for each j-th time moment is determined using the 1^{st} Fick's law. This is possible thanks to the numerically computed total flux $h(\tau_j)$ through the boundary. We suppose the symmetry, hence the total flux is equally divided into the left border ($x = 0$) and the right border ($x = 1$), see later for more details.

Recall that due to the measurement noise both the respective $j-$ *profiles* $y_{exp}(x_i, \tau_j),\ i = 0 \dots N$, and the initial and boundary conditions cannot be simply approximated by a smooth function. The forthcoming task is to analyze the measurement noise from real data and to treat it correctly.

Outline

Objective function

We construct an objective function J representing the disparity between the experimental and simulated time-varying concentration profiles, and then within a suitable method we look for such a value p minimizing J.

The usual form of an objective function is the sum of squared differences between the experimentally measured and numerically simulated time-varying concentration profiles:

$$J(p) = \sum_{j=0}^{M} \sum_{i=0}^{N} \left[y_{exp}(x_i, \tau_j) - y_{sim}(x_i, \tau_j, p) \right]^2 , \tag{8}$$

where $y_{sim}(x_i, \tau_j, p)$ are the simulated values resulting from the solution of problem (4)–(6).

Biological reality

Taking into account the biological reality residing in possible time dependence of phycobilins diffusivity, for the minimization problem

$$\min_p J(p) = \min_p \sum_{j=0}^{M} \sum_{i=0}^{N} [y_{exp}(x_i, \tau_j) - y_{sim}(x_i, \tau_j, p)]^2 \qquad (9)$$

we further consider two cases:

1. We can take both sums for i and j in (9) together. In this case, the scalar p is a result of minimization problem for J.
2. We can consider each j-th time column separately. In this case, the M solutions $p_1 \dots p_M$ correspond to each minimization problem for fixed j in sum (9) and we have a 'dynamics' of diffusivity p evolution.

Data *P. Cruentum - 11-11 14*: diffusion coefficients p_j

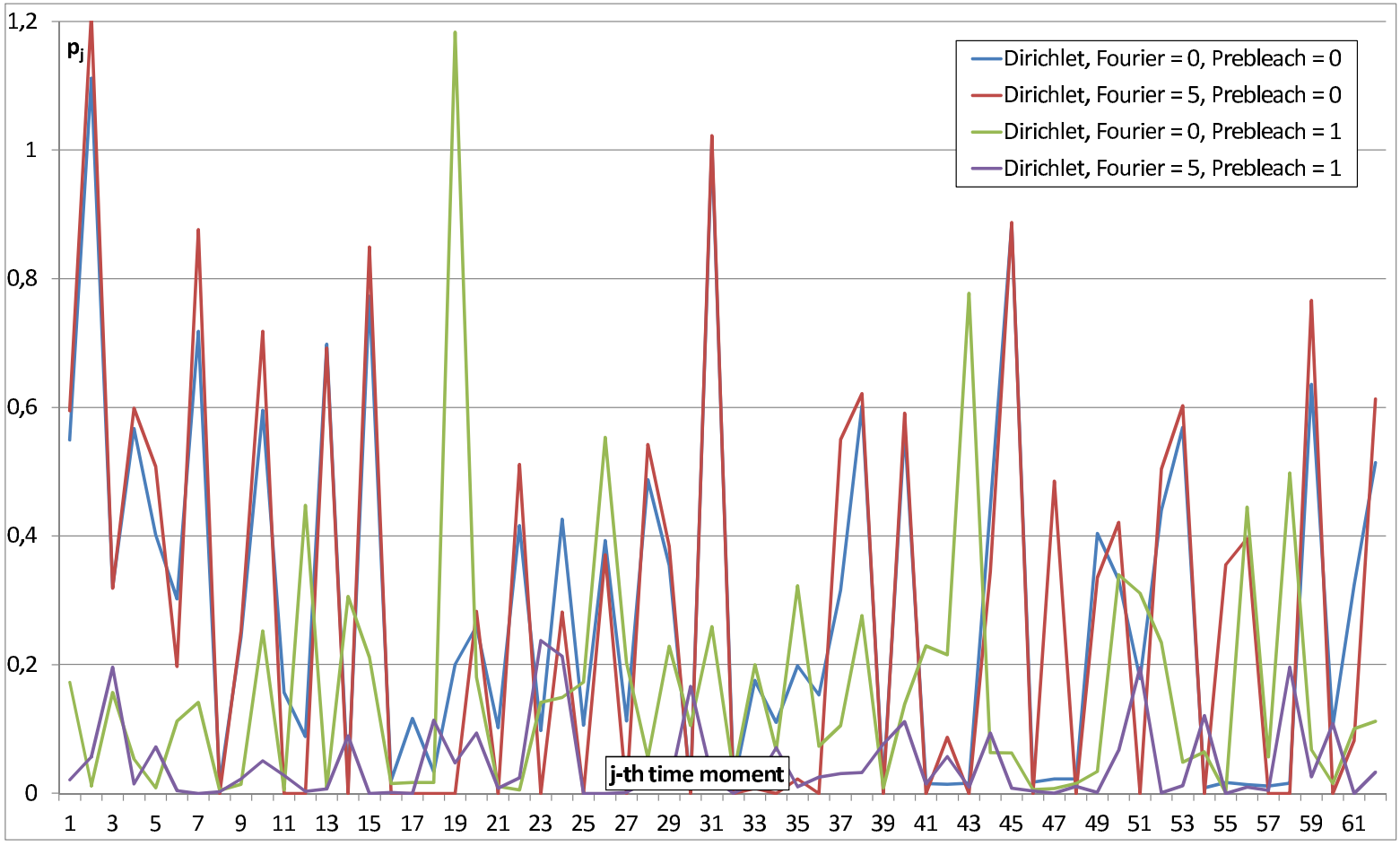

Test data: diffusion coefficients p_j

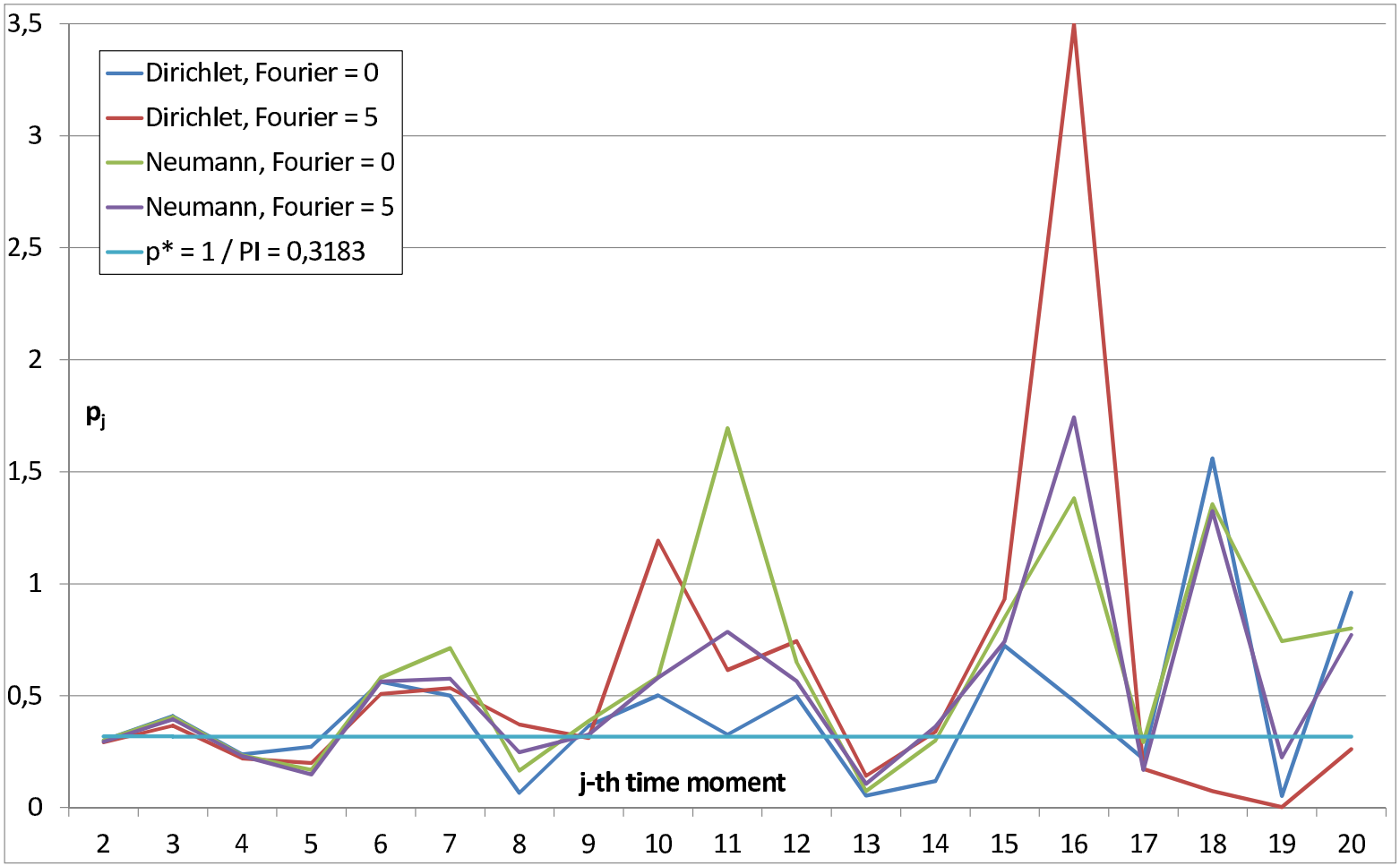

Outline

Abstract formulation

We assume model in form of

$$T(p) = f$$

and we want to find

$$p = T^{-1}(f)\,.$$

Abstract formulation

We assume model in form of

$$T(p) = f$$

and we want to find

$$p = T^{-1}(f)\,.$$

Operator T is not analytically invertible, therefore we want to find

$$p^* = \arg\min_p ||\,T(p) - f\,||^2\,.$$

Abstract formulation

We assume model in form of

$$T(p) = f$$

and we want to find

$$p = T^{-1}(f)\,.$$

Operator T is not analytically invertible, therefore we want to find

$$p^* = \arg\min_p ||\,T(p) - f\,||^2\,.$$

In reality we have only approximation of T – $\widetilde{T}$ and we don't have the exact data – $f = f_{exact} + f_{noise}$ and therefore we obtain

$$\widetilde{p}^* = \arg\min_p ||\,\widetilde{T}(p) - f_{exact} + f_{noise}||^2\,.$$

Minimum of the functional $\widetilde{p}^*$ can be very far from exact p.

Example - backward heat equation 1

Let consider for simplicity we solve the heat equation with homogenous BC at $(-\infty, +\infty) \times (0, +\infty)$

$$\frac{\partial y}{\partial \tau} - p \frac{\partial^2 y}{\partial x^2} = 0$$

with initial condition

$$y(x, \tau_0) = f(x), \quad x \in (-\infty, +\infty)\,. \tag{10}$$

Example - backward heat equation 1

Let consider for simplicity we solve the heat equation with homogenous BC at $(-\infty, +\infty) \times (0, +\infty)$

$$\frac{\partial y}{\partial \tau} - p \frac{\partial^2 y}{\partial x^2} = 0$$

with initial condition

$$y(x, \tau_0) = f(x), \quad x \in (-\infty, +\infty)\,. \tag{10}$$

Solution of this problem is

$$y(x, \tau) = (T(f) =) \int_{-\infty}^{\infty} K_{p\tau}(x - y) f(y) dy\,, \tag{11}$$

where $K_\tau(x) = \frac{1}{4\pi\tau} \exp(-\frac{x^2}{4\tau})$.

Example - backward heat equation 1

Let consider for simplicity we solve the heat equation with homogenous BC at $(-\infty, +\infty) \times (0, +\infty)$

$$\frac{\partial y}{\partial \tau} - p \frac{\partial^2 y}{\partial x^2} = 0$$

with initial condition

$$y(x, \tau_0) = f(x), \quad x \in (-\infty, +\infty)\,. \tag{10}$$

Solution of this problem is

$$y(x, \tau) = (T(f) =) \int_{-\infty}^{\infty} K_{p\tau}(x - y) f(y) dy\,, \tag{11}$$

where $K_\tau(x) = \frac{1}{4\pi\tau} \exp(-\frac{x^2}{4\tau})$.
When we know the final state and searching IC, we solve the Fredholm integral equation of first kind. Operator T is compact, linear and its spectrum is discrete with cumulative point at 0.

Example - backward heat equation 2

Compact linear operators can be written in the form of singular value expansion

$$T(x) = \sum_{i=1}^{+\infty} \sigma_i \langle x, v_i \rangle u_i \,, \tag{12}$$

where u_i (v_i) are a complete orthonormal system of eigenvectors of TT^* (T^*T).

Example - backward heat equation 2

Compact linear operators can be written in the form of singular value expansion

$$T(x) = \sum_{i=1}^{+\infty} \sigma_i \langle x, v_i \rangle u_i \,, \tag{12}$$

where u_i (v_i) are a complete orthonormal system of eigenvectors of TT^* (T^*T).
For some y we can find pseudoinverse $T^\dagger$ of form

$$T^\dagger(y) = \sum_{i=1}^{+\infty} \frac{\langle y, u_i \rangle}{\sigma_i} v_i \,, \tag{13}$$

which satisfies $T^\dagger = (T|_{N(T)^\perp})^{-1}$.

Example - backward heat equation 2

Compact linear operators can be written in the form of singular value expansion

$$T(x) = \sum_{i=1}^{+\infty} \sigma_i \langle x, v_i \rangle u_i \,, \tag{12}$$

where u_i (v_i) are a complete orthonormal system of eigenvectors of TT^* (T^*T).
For some y we can find pseudoinverse $T^\dagger$ of form

$$T^\dagger(y) = \sum_{i=1}^{+\infty} \frac{\langle y, u_i \rangle}{\sigma_i} v_i \,, \tag{13}$$

which satisfies $T^\dagger = (T|_{N(T)^\perp})^{-1}$.
Operator $T^\dagger$ is unbounded. Noise in y can completely overlay the correct information.

Example - differentiation

Let $f \in C^1[0,1]$ be any function, $\delta \in (0,1)$, $n \in N$ $(n \geq 2)$ be arbitrary and define

$$f_n^\delta(x) := f(x) + \delta \sin \frac{nx}{\delta}, \quad x \in [0,1]\,. \tag{14}$$

Then

$$(f_n^\delta)'(x) := f'(x) + n \cos \frac{nx}{\delta}, \quad x \in [0,1]\,. \tag{15}$$

Example - differentiation

Let $f \in C^1[0,1]$ be any function, $\delta \in (0,1)$, $n \in N$ $(n \geq 2)$ be arbitrary and define

$$f_n^\delta(x) := f(x) + \delta \sin \frac{nx}{\delta}, \quad x \in [0,1]\,. \tag{14}$$

Then

$$(f_n^\delta)'(x) := f'(x) + n \cos \frac{nx}{\delta}, \quad x \in [0,1]\,. \tag{15}$$

Now, in the uniform norm,

$$||f - (f_n^\delta)||_\infty = \delta\,, \tag{16}$$

but

$$||f' - (f_n^\delta)'||_\infty = n\,. \tag{17}$$

Example - differentiation

Let $f \in C^1[0,1]$ be any function, $\delta \in (0,1)$, $n \in N$ $(n \geq 2)$ be arbitrary and define

$$f_n^\delta(x) := f(x) + \delta \sin \frac{nx}{\delta}, \quad x \in [0,1]\,. \tag{14}$$

Then

$$(f_n^\delta)'(x) := f'(x) + n \cos \frac{nx}{\delta}, \quad x \in [0,1]\,. \tag{15}$$

Now, in the uniform norm,

$$||f - (f_n^\delta)||_\infty = \delta\,, \tag{16}$$

but

$$||f' - (f_n^\delta)'||_\infty = n\,. \tag{17}$$

We can see, that the derivative does not depend continuously on the data with respect to the uniform norm.

From similar reasons our parameter identification problem

$$\widetilde{p}^* = \arg\min_p ||\widetilde{T}(p) - f_{exact} + f_{noise}||^2$$

may not depend continuously on the data and may be very sensitive to noise f_{noise}.

From similar reasons our parameter identification problem

$$\widetilde{p}^* = \arg\min_p ||\widetilde{T}(p) - f_{exact} + f_{noise}||^2$$

may not depend continuously on the data and may be very sensitive to noise f_{noise}.
Therefore we regularize the problem by adding the regularization term

$$\alpha||p - p_{reg}||^2 .$$

We assume that $p(x, \tau)$ is almost constant with respect to x and τ and regularization term moves the minimum of functional $\widetilde{p}^*$ towards a constant function. In case $\alpha \to \infty$ we obtain $\widetilde{p}^* = p_{reg}$.
We minimize new functional with respect to p and p_{reg}

$$\widetilde{p}^* = \arg\min_{p, p_{reg}} (||\widetilde{T}(p) - f_{exact} + f_{noise}||^2 + \alpha||p - p_{reg}||^2) .$$

Outline

Appropriate approach

Our problem is ill-posed in the sense that the solution, i.e. the diffusion coefficients

$$D_j = p_j D_0, \quad j = 1 \dots M$$

do not depend continuously on the initial experimental data. This led us to the necessity of using some stabilizing procedure:

- Naive approach: To remove the noise in experimental values, consider their smoothing by using the Fourier transformation.
- Appropriate approach: Formulation of regularized cost functions:

$$J_j(p, \alpha) = \sum_{i=0}^{N} \left[y_{exp}(x_i, \tau_j) - y_{sim}(x_i, \tau_j, p) \right]^2 + \alpha \left(p - p_{reg} \right)^2 \qquad (18)$$

for $j = 1 \dots M$, where $\alpha \geq 0$ is a regularization parameter, and p_{reg} is an expected value.

Taking $\alpha = 0$, function $J(p) = \sum_{j=0}^{M} J_j(p, 0)$ turns to (8).

Optimization problem

Minimizing J with respect to $p > 0$ represents a one-dimensional optimization problem. Three types are considered:

1. Scalar p is a solution when taking both sums for i and j in together:

$$p^* = \arg\min_p \sum_{j=0}^{M} \sum_{i=0}^{N} \left[y_{exp}(x_i, \tau_j) - y_{sim}(x_i, \tau_j, p) \right]^2$$

2. Each j-th time column separately without regularization ($\alpha = 0$)

$$p_j = \arg\min_p \sum_{i=0}^{N} \left[y_{exp}(x_i, \tau_j) - y_{sim}(x_i, \tau_j, p) \right]^2$$

3. Each j-th time column separately using Tikhonov regularization

$$p_j(\alpha) = \arg\min_p \left\{ \sum_{i=0}^{N} \left[y_{exp}(x_i, \tau_j) - y_{sim}(x_i, \tau_j, p) \right]^2 + \alpha \left(p - p_{reg} \right)^2 \right\}$$

We use a basic optimization method leading to values p^*, p_j, $p_j(\alpha)$ that minimize J. Values p_j, $p_j(\alpha)$ are approximations of diffusion coefficients.

Basic optimization method

Basic optimization method is an iteration process starting from an initial point $p^{(0)}$ and generating a sequence of iterates $p^{(1)}, p^{(2)}, \ldots$ leading to a value p^* such that

$$p^{(l+1)} = p^{(l)} + \sigma^{(l)} d^{(l)},$$

where

- $d^{(l)}$ is a direction vector – is determined on the basis of values

$$p^{(j)},\ J(p^{(j)}),\ J'(p^{(j)}),\ J''(p^{(j)}), \quad 0 \leq j \leq l,$$

- $\sigma^{(l)} > 0$ is a step-length – is determined on the basis of behavior of the function J in the neighborhood of $p^{(l)}$.

We use a suitable optimization method from the so-called UFO system

http://www.cs.cas.cz/luksan/ufo.html

Problem to be solved

In order to compute a function value $J_j(p^{(l)}, \alpha)$ in (18) for a given $p^{(l)}$ in the l-th iteration, we need to know both

- the experimental values $y_{exp}(x_i, \tau_j),\ i = 0 \ldots N,\ j = 0 \ldots M,$
- the simulated values $y_{sim}(x_i, \tau_j, p^{(l)}),\ i = 0 \ldots N,\ j = 0 \ldots M.$

It means that in each l-th iteration we need to solve the problem (let put $y_{sim} \equiv y,\ p^{(l)} \equiv p$ for simplicity)

$$\frac{\partial y}{\partial \tau} - p \frac{\partial^2 y}{\partial x^2} = 0 \tag{19}$$

with the initial and boundary conditions defined by the experimental data:

$$y(x, \tau_0) = y_{exp}(x, \tau_0), \quad x \in [0, 1] \tag{20}$$

$$\textbf{(D)} \qquad y(0, \tau) = y_{exp}(0, \tau), \qquad y(1, \tau) = y_{exp}(1, \tau), \qquad \tau \geq \tau_0 \tag{21}$$

$$\textbf{(N)} \qquad -py'(0, \tau) = \frac{Flux(\tau)}{2}, \quad py'(1, \tau) = \frac{Flux(\tau)}{2}, \quad \tau \geq \tau_0 \tag{22}$$

Simulated data

Problem (19)-(22) for simulated data $y(x_i, \tau_j)$ was solved numerically using the finite difference scheme for uniformly distributed nodes with the space steplength Δh and the variable time steplength $\Delta\tau$:

1. The explicit scheme of order $\Delta\tau + \Delta h^2$:

$$y_{i,j} = \beta y_{i-1,j-1} + (1 - 2\beta) y_{i,j-1} + \beta y_{i+1,j-1}$$

2. The Crank-Nicholson implicit scheme of order $\Delta\tau^2 + \Delta h^2$:

$$-\frac{\beta}{2} y_{i-1,j} + (1+\beta) y_{i,j} - \frac{\beta}{2} y_{i+1,j} = \frac{\beta}{2} y_{i-1,j-1} + (1-\beta) y_{i,j-1} + \frac{\beta}{2} y_{i+1,j-1}$$

Here $\beta = \frac{\Delta\tau}{\Delta h^2}\, p$ and $y_{i,j} \equiv y(x_i, \tau_j)$ are the computed values in nodes that enter the function J as values $y_{sim}(x_i, \tau_j)$.

Recall that for the explicit scheme the condition $\beta \leq 1/2$ must hold.

Space and time steplengths

Steplengths used in the numerical scheme:

- Space steplength: $\Delta h = 1/N$ or $\Delta h = 1/(\kappa_s N),\ \kappa_s \in \mathbb{N}$
- Time steplength: $\Delta\tau$ should be ideally of the same order as Δh^2 (or Δh in the CN scheme) and in the explicit scheme has to fulfill the relation $\Delta\tau \leq \frac{\Delta h^2}{2p}$.

In order to get from the $(j-1)$-th time column to the j-th, we need to perform

$$\kappa_t = \frac{TD_0}{L^2\Delta\tau}$$

substeps, where $\kappa_t \in \mathbb{N}$ has to be an integer depending on $\Delta\tau$.

Differential scheme

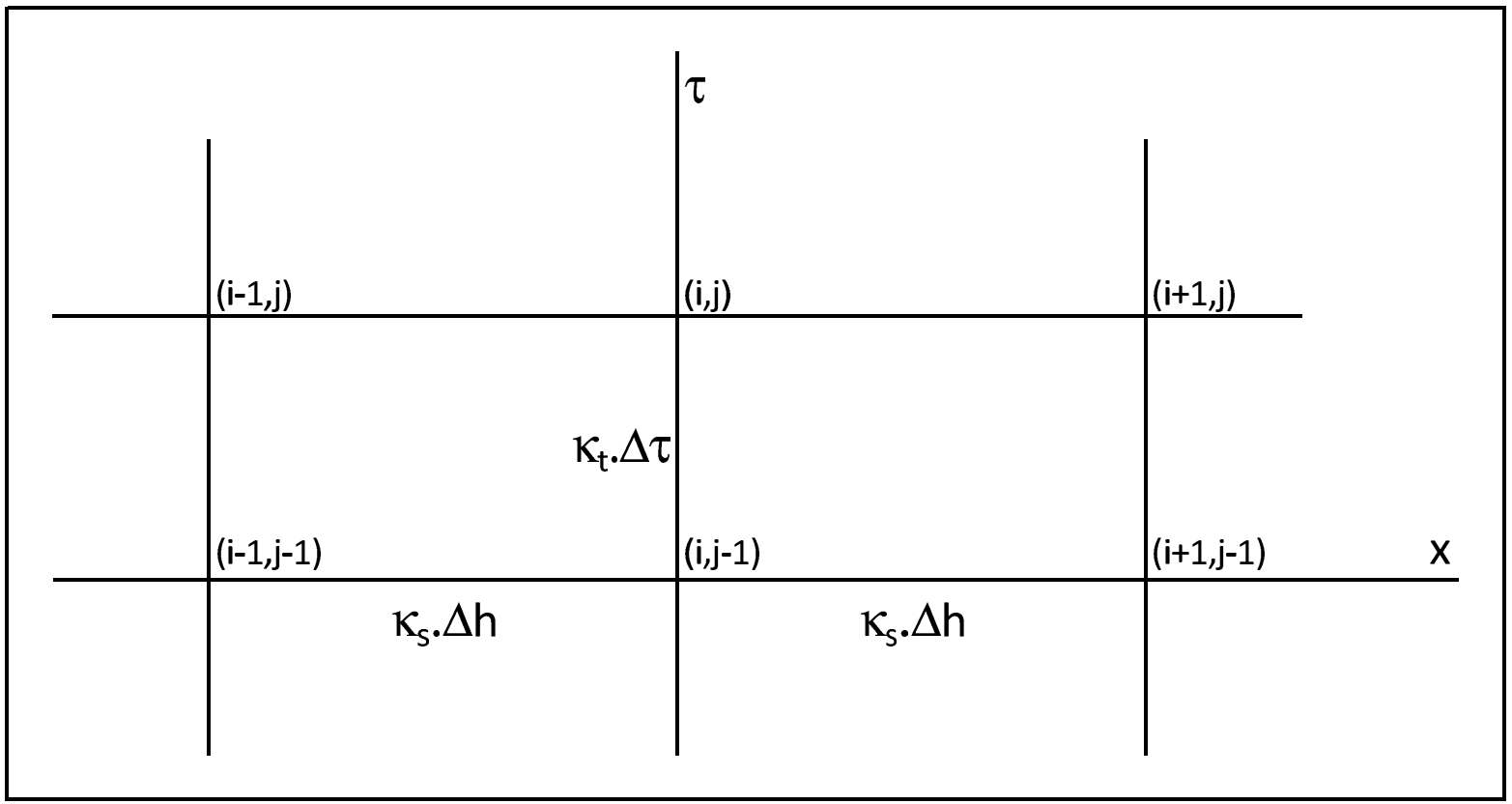

Neumann boundary conditions

When considering the Neumann BC, we use the following formulas:

$$-\frac{Flux(j)}{2p} = y'(0,\tau_j) = y'(x_0,\tau_j) \approx$$

1. $$\frac{y_{exp}(x_1,\tau_j) - y_{exp}(x_{-1},\tau_j)}{2\Delta h}$$

2. $$\frac{-y_{exp}(x_2,.) + 8y_{exp}(x_1,.) - 8y_{exp}(x_{-1},.) + y_{exp}(x_{-2},.)}{12\Delta h}$$

3. $$\frac{-3y_{exp}(x_4) + 16y_{exp}(x_3) - 36y_{exp}(x_2) + 48y_{exp}(x_1) - 25y_{exp}(x_0)}{12\Delta h}$$

and similarly on the other side:

$$\frac{Flux(j)}{2p} = y'(1,\tau_j) = y'(x_N,\tau_j) \approx \ldots$$

The errors are: $\frac{\Delta h^2}{6}\, y^{(3)}$, $\frac{\Delta h^4}{30}\, y^{(5)}$, $\frac{\Delta h^4}{5}\, y^{(5)}$.

Computing the flow or flux through the border $\partial\Omega$

To compute the diffusive flux $J(r,t)$, we use the Fick's first law

$$-D\,\nabla C(r,t) = J(r,t) \quad \text{on} \quad \partial\Omega \times [t_0, T].$$

Further, we use the term $Flux(j)$ for the total flux through the border, based on mass balance we have

$$Flux(j) = \frac{\partial}{\partial t}\int_{\Omega} C(r,t)\mathrm{d}V.$$

In our 1D case, we compute for each j^{th} moment

$$y_{sum}(j) = \mathrm{sstep}\left[\frac{y_{exp}(x_0,\tau_j) + y_{exp}(x_N,\tau_j)}{2} + \sum_{i=1}^{N-1} y_{exp}(x_i,\tau_j)\right]$$

and set

$$Flux(j) = \frac{\mathrm{LC}\{y_{sum}(j-2), y_{sum}(j-1), y_{sum}(j+1), y_{sum}(j+2)\}}{\mathrm{tstep}}$$

where

- sstep is a space step between two experimental data
- tstep is a time step between two experimental data

Outline

Tikhonov regularization

Values p_j and $p_j(\alpha)$ are approximate solutions of minimization problems

$$p_j = \arg\min_p J_j(p), \quad p_j(\alpha) = \arg\min_p J_j(p, \alpha)$$

It holds

$$\lim_{\alpha \to 0} p_j(\alpha) = p_j$$

What we have for $\alpha \to \infty$:

:-) solutions $p_j(\alpha)$ are more and more constant i.e. $p_j(\alpha) \equiv p_{reg}\ \forall j$

:-(function value $J_j(p_j(\alpha), \alpha)$ becomes larger (they have a limit point)

We look for such a value α^* for which the relative standard deviation is small enough.

L-curve criterion

Criterion called the L-curve:
We plot

- the value of objective function J (without the regularization term)

against

- the average value $\emptyset p_j(\alpha)$ and the deviation of $p_j(\alpha)$ from $\emptyset p_j(\alpha)$ (or construct a combination when we know the exact solution)

The L-curve optimal parameter α^* then corresponds to the point with maximal curvature.

For the plotting we use the following quantities:

1. Objective function J

$$J(p_1(\alpha)\dots p_M(\alpha)) = \sum_{j=0}^{M}\sum_{i=0}^{N}\left[y_{exp}(x_i,\tau_j) - y_{sim}(x_i,\tau_j,p_j(\alpha))\right]^2$$

2. „Relative“ deviation from the average value
(so-called coefficient of variation)

$$\sigma = \frac{1}{M\not{o}p_j(\alpha)}\sqrt{\sum_{j=1}^{M}[p_j(\alpha) - \not{o}p_j(\alpha)]^2}$$

3. Relative deviation from the solution

$$\omega = \frac{|\not{o}p_j(\alpha) - p^*| + \sigma}{p^*}$$

The algorithm

For a fixed regularization parameter α we determine diffusion coefficients $p_1(\alpha) \dots p_M(\alpha)$ in the following way:

1. Choose initial expected value p_{reg} and stopping tolerance ε_{reg}
2. Compute $p_j(\alpha),\ j = 1 \dots M$, by minimizing functions

$$J_j(p, \alpha) = \left\{ \sum_{i=0}^{N} \left[y_{exp}(x_i, \tau_j) - y_{sim}(x_i, \tau_j, p) \right]^2 + \alpha \left(p - p_{reg} \right)^2 \right\}$$

3. Compute the average value

$$\emptyset p_j(\alpha) = \frac{p_1(\alpha) + \dots + p_M(\alpha)}{M}$$

4. If

$$\left| \emptyset p_j(\alpha) - p_{reg} \right| \leq \varepsilon_{reg},$$

   then STOP.
5. Set $p_{reg} = \emptyset p_j(\alpha)$ and go back to step 2.

Outline

Test data

Dirichlet boundary condition, noise $= 1\%, 5\%, 10\%, 20\%$:
j-th time moment against values p_j for different α

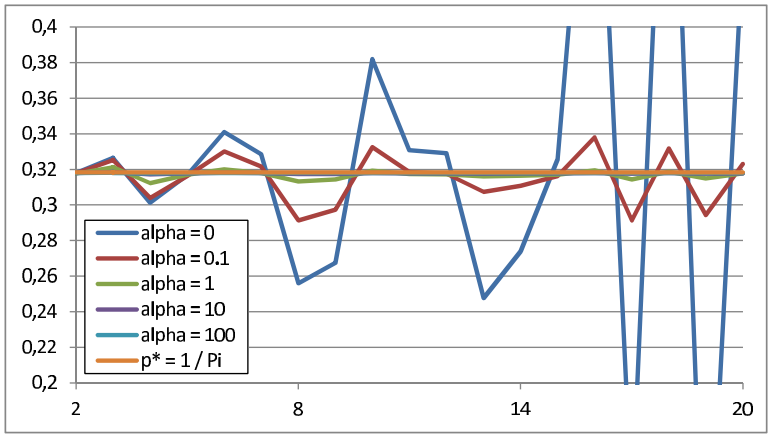

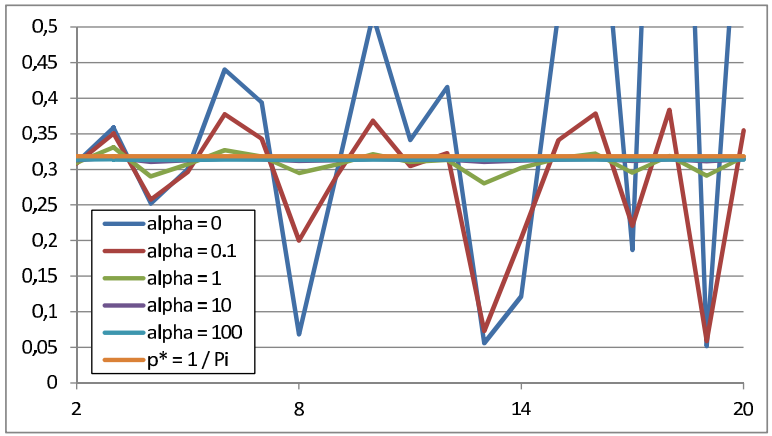

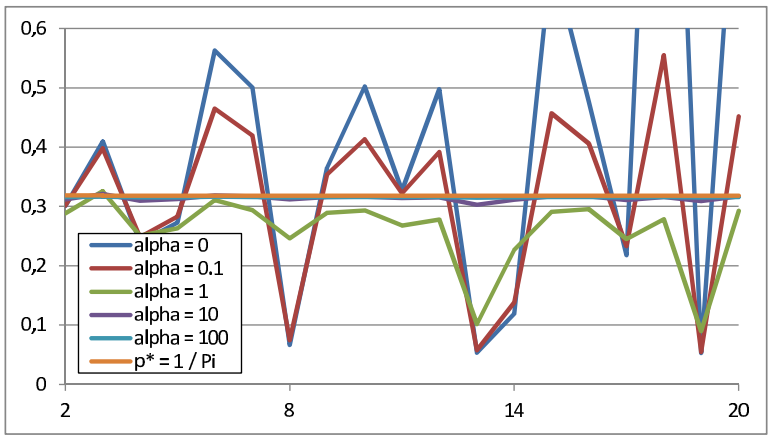

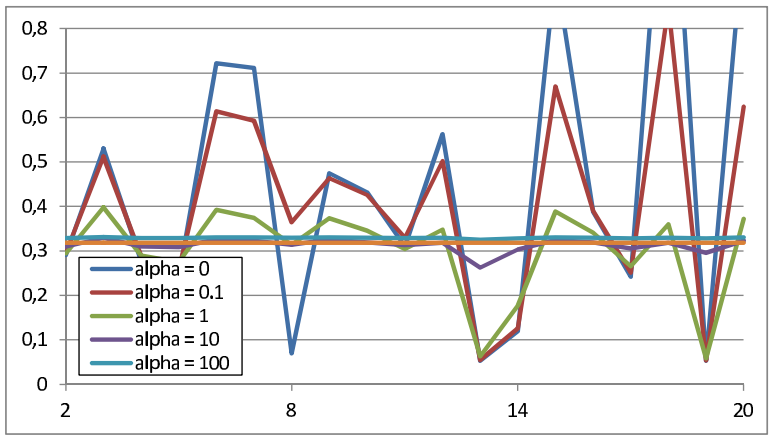

Test data

Neumann boundary condition, noise $= 1\%, 5\%, 10\%, 20\%$:
j-th time moment against values p_j for different α

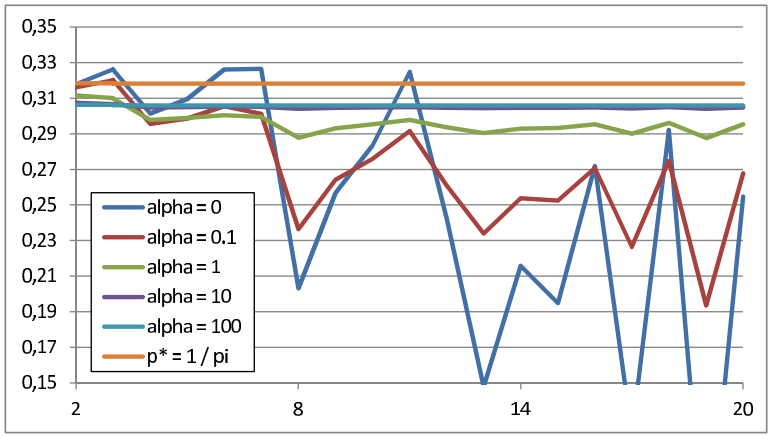

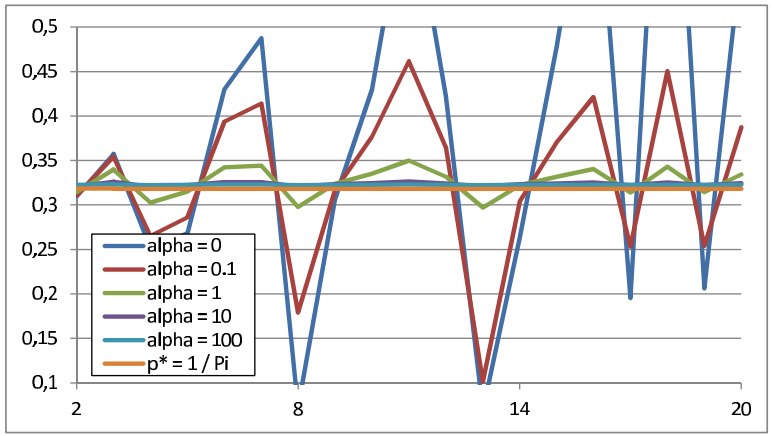

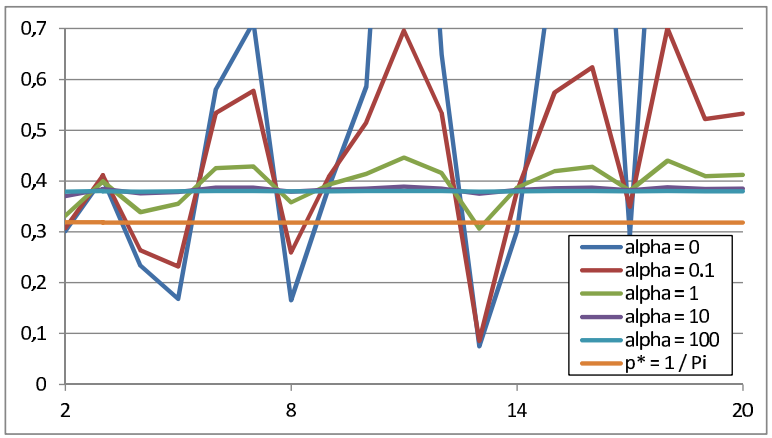

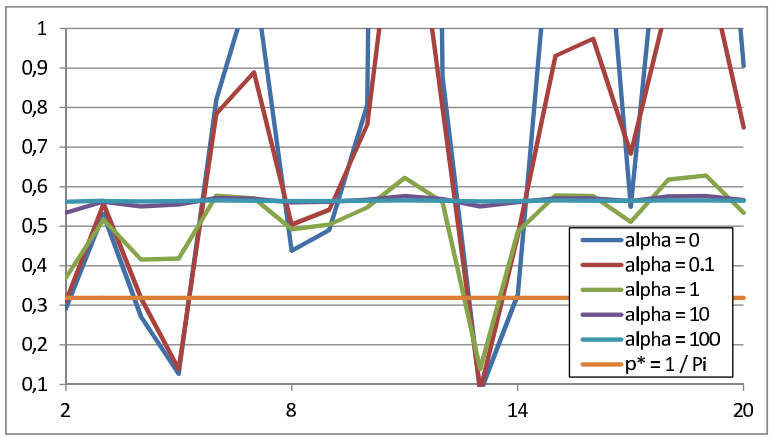

Test data

Dirichlet boundary condition, noise $= 1\%, 5\%, 10\%, 20\%$:
L-curve – values J against values ω
$\alpha = 0$, 1d-4, 1d-3, 1d-2, 1d-1, 5d-1, 1, 5, 10, 50, 100, 500

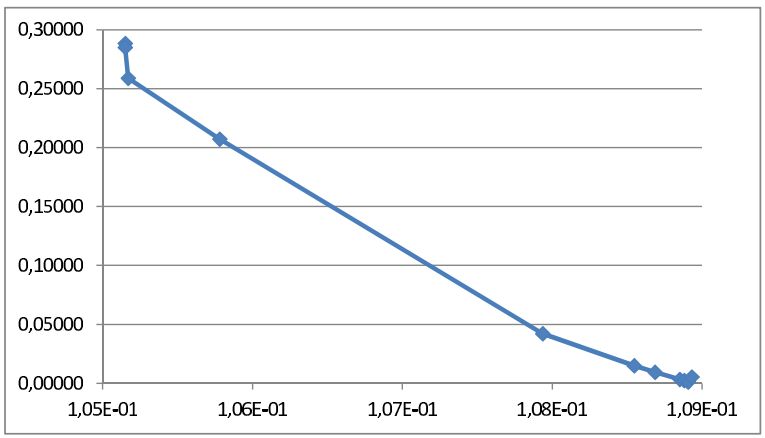

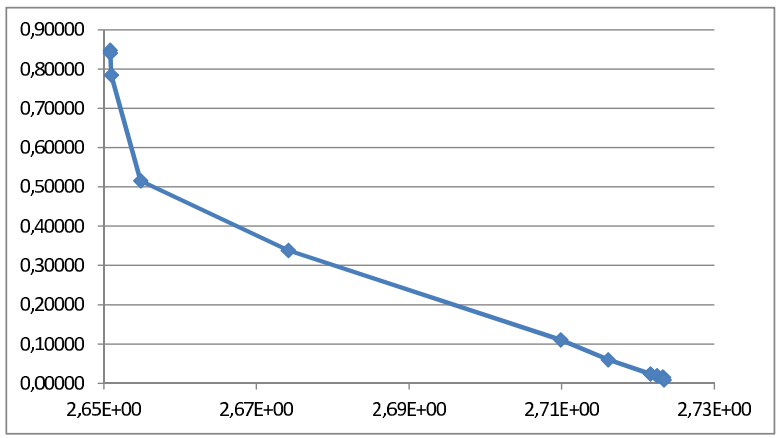

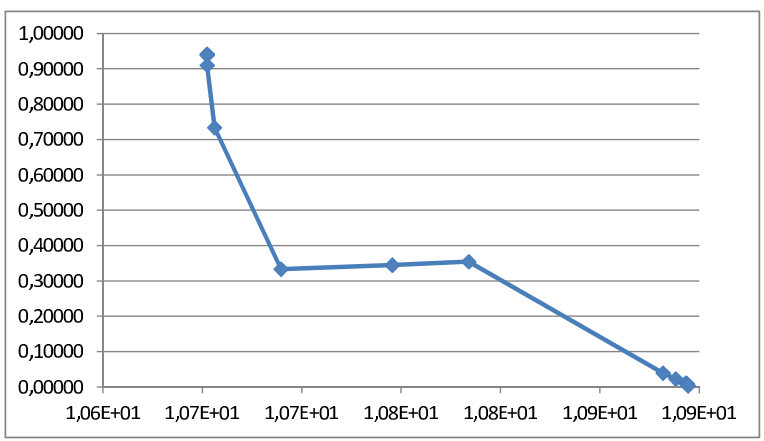

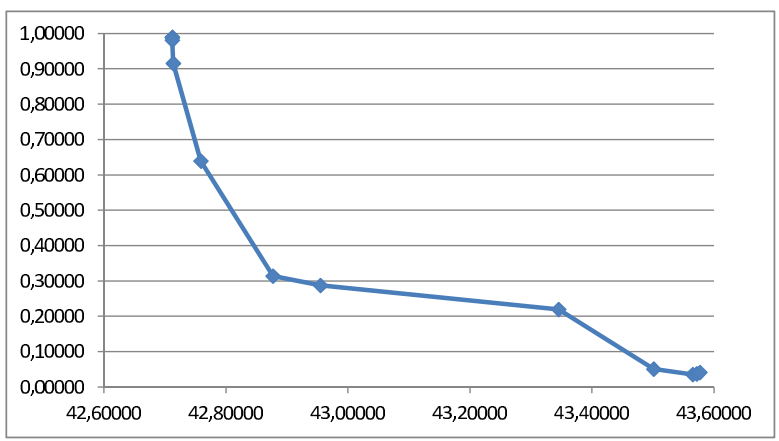

Test data

Neumann boundary condition, noise $= 1\%, 5\%, 10\%, 20\%$:
L-curve – values J against values ω
$\alpha = 0$, 1d-4, 1d-3, 1d-2, 1d-1, 5d-1, 1, 5, 10, 50, 100, 500

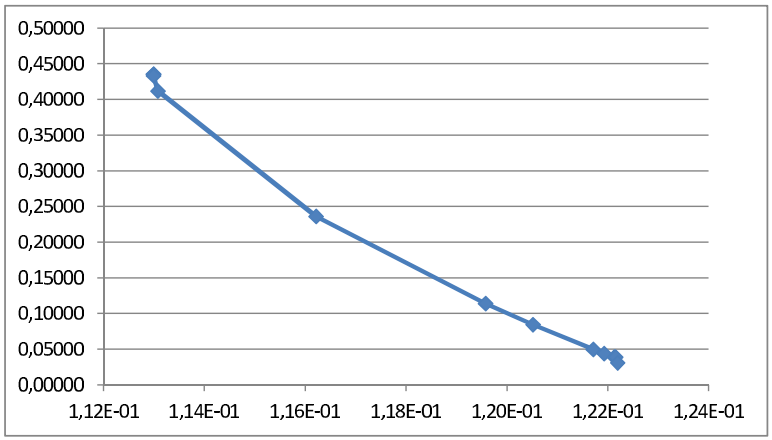

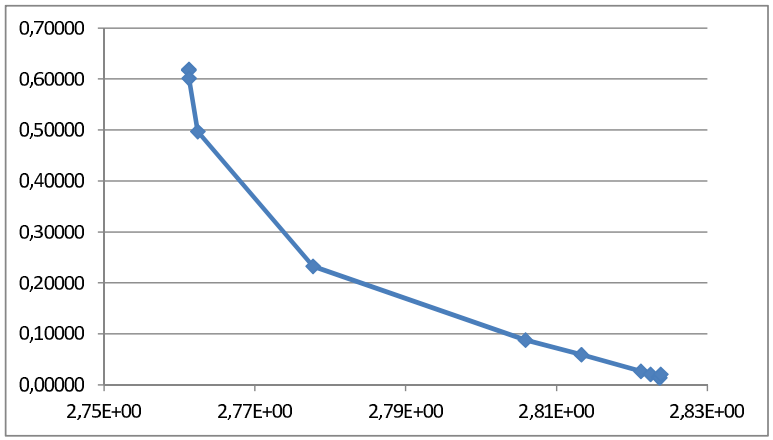

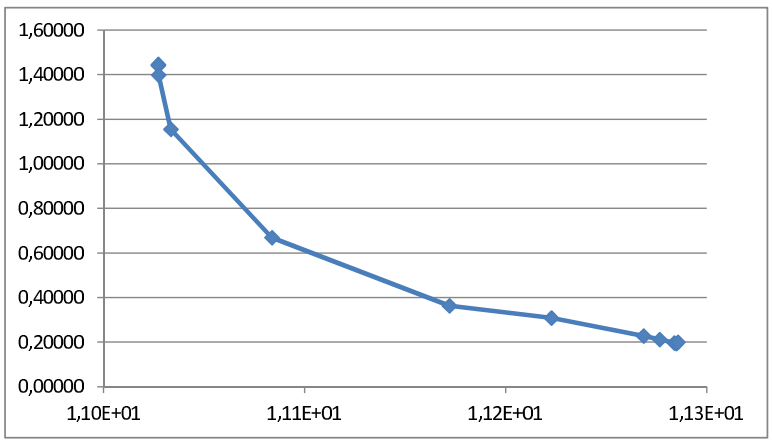

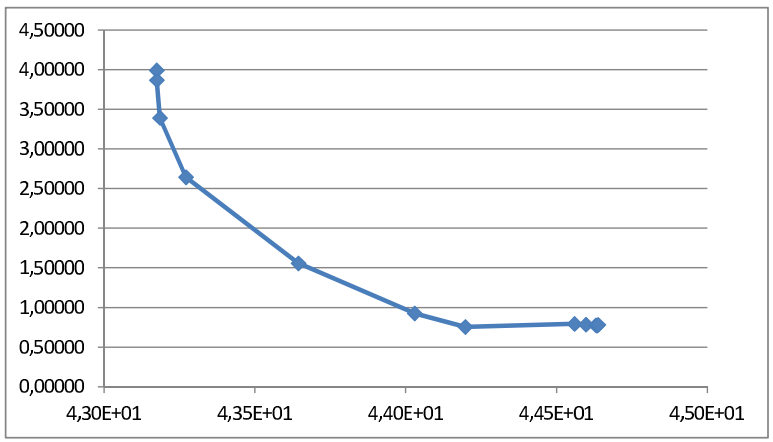

Test data

Values p_j for Dirichlet (UL) and Neumann (UR) boundary conditions;
values of *deviation* for Dirichlet (BL) and Neumann (BR) b.c.

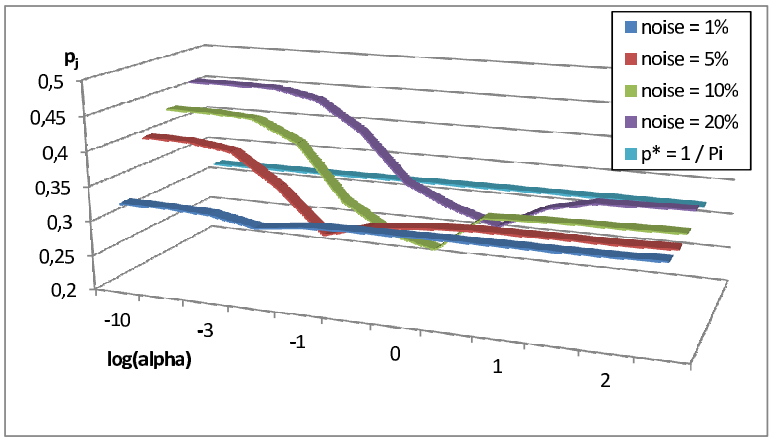

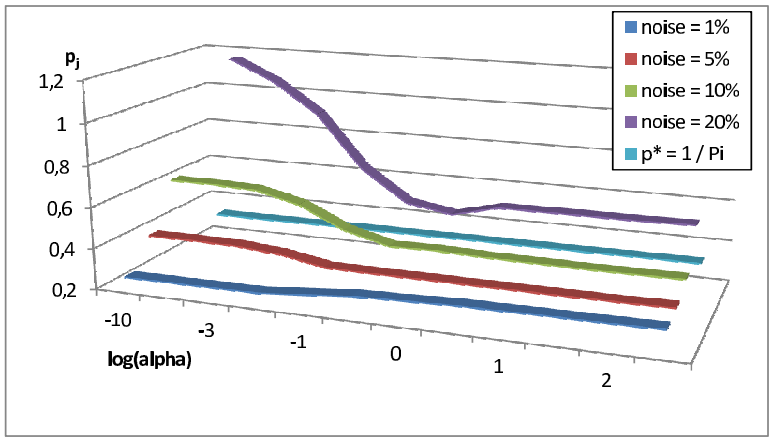

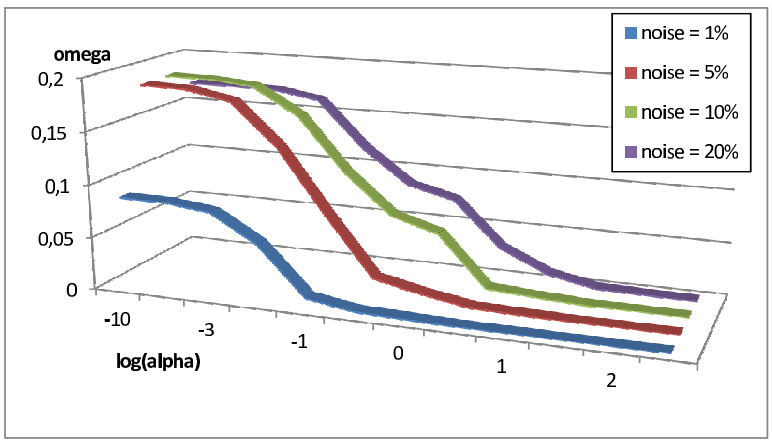

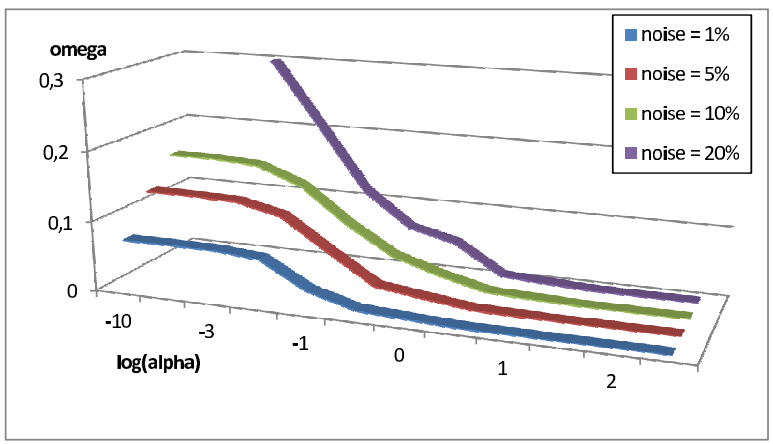

Conclusion

- Our method improves on other models by accounting for experimentally measured post-bleaching fluorescence profiles and time-dependent boundary conditions, and can include also a reaction term to account for the low level bleaching during scanning and the time varying fluorescence signal.
- Finding an optimal solution p is quite a difficult task. We would like to improve our method by an adequate assessment of the measurement noise and by an implementation of a suitable regularization technique and a more robust optimization procedure.
- For the previously known diffusion coefficient and the data simulated by the random walk model our program computes correct results. We determined the diffusivities for the real data of FRAP measurements (with the red algae *Porphyridium cruentum*). The range of result $10^{-14}\mathrm{m}^2\mathrm{s}^{-1}$ is in agreement with reference values.

References

- Moullineaux C.W., Tobin M.J., Jones G.R.:
  Mobility of photosynthetic complexes in thylakoid membranes.
  Nature, 390 (1997), 421-–424.
- Papáček Š., Štys D., Kaňa R., Matonoha C.:
  Parameter estimation of reaction-diffusion model based on spatio-temporal FRAP images of thylakoid membranes.
  Proceedings of seminar „SNA'11“, Rožnov pR 2011, p. 92-95
- Papáček Š., Matonoha C.:
  Analysis of phycobilisomes mobility on thylakoid membrane.
  Proceedings of seminar „Matematika na vysokých školách“, Herbertov, 2011, p. 63-70
- Papáček Š., Kaňa R., Matonoha C.:
  Estimation of diffusivity of phycobilisomes on thylakoid membrane based on spatio-temporal FRAP images.
  Technical report V1123, ICS AS CR, Prague, 2011;
  In: L. Jódar, L. Acedo, J.C. Cortés, IUMM (Ed.), Modelling for engineering and human behaviour 2011 (book of extended abstracts), Valencia 2011, p. 248-251;
  Mathematical and Computer Modelling (accepted)
- Papáček Š., Kaňa R., Matonoha C.:
  Estimation of diffusivity of phycobilisomes on thylakoid membrane based on spatio-temporal FRAP images.
  Proceedings of seminar „SNA'12“, Liberec 2012, p. 146-148